DOI: 10.4274/jcrpe.galenos.2025.2025-1-18

Research Article

Diagnostic Utility in Next-Generation Sequencing by Implicating CNV Analysis in Eleven Patients with Peters Plus Syndrome: A Single-Center Experience

Akalın A et al. Diagnostic Utility in Next-Generation Sequencing by Implicating CNV Analysis in Peters Plus Syndrome

Akçahan Akalın[1], Enise Avcı Durmuşalioğlu[2], Şervan Özkalkak[3], Ruken Yıldırım[3], Veysel Öz[4], Edip Ünal[5], Leyla Hazar[6], Türkan Turkut Tan[2], Yusuf Can Doğan[2], Tahir Atik[2], Özgür Çoğulu[2], Esra Işık[2]
[1]Department of Pediatric Genetics, Diyarbakir Children's Hospital, Diyarbakır, Turkey
[2]Division of Pediatric Genetics, Department of Pediatrics, School of Medicine, Ege University, Izmir, Turkey
[3]Department of Pediatric Endocrinology, Diyarbakir Children's Hospital, Diyarbakır, Turkey
[4]Department of Pediatric Neurology, Diyarbakir Children's Hospital, Diyarbakır, Turkey
[5]Department of Pediatric Endocrinology, Dicle University, Faculty of Medicine, Diyarbakır, Turkey
[6]Department of Ophthalmology, Dicle University, Faculty of Medicine, Diyarbakır, Turkey

What is already known on this topic?
• PTRPLS syndrome is a rare genetic condition caused by biallelic pathogenic variants in the B3GLCT gene.
• Affected individuals exhibited anterior eye-chamber defects, disproportionate short stature, and facial dysmorphism.

What this study adds?
• To the best of our knowledge, this is the first report demonstrating that exonic deletions can contribute to the pathogenesis of PTRPLS.
• We report the smallest homozygous deletion identified on chromosome 13q12, encompassing the 15th exons of the B3GLCT gene in PTRPLS patients.

Abstract
Objective: Peters Plus syndrome (PTRPLS**)** is an autosomal recessive congenital disorder of glycosylation caused by biallelic pathogenic variants in the ß 1,3-glucosyltransferase gene (B3GLCT). To date, homozygous or compound heterozygous splicing, truncating, missense variants, and whole gene deletions have been reported in the B3GLCT gene. This study aims to emphasize the role of small copy number variations (CNVs) in this condition alongside the clinical features of the patients.
Methods: The study included eleven patients from six consanguineous families originating from the same village. Clinical exome sequencing-based CNV analysis was employed across all probands to ascertain the genetic background.
Results: Using GATK-gCNV, we identified a homozygous deletion on chromosome 13q12.3, encompassing 15th exon of the B3GLCT gene. The mean age at admission was 9.6 ± 13.3 years, ranging from 2 months to 41 years. The mean standart deviation (SD) scores for height and weight at admission were -4.4 ± 0.9 and -3.8 ± 1.8, respectively. Ophthalmological abnormalities included corneal haze, anterior synechiae, unilateral leucoma, corneal-lenticular adhesion, glaucoma, and severe visual loss. Patients under the age of five exhibited global developmental delay, while those older than five years demonstrated varying degrees of intellectual disability, with two exceptions exhibiting normal cognitive function.
Conclusion: Our findings underscore the critical role of NGS-based CNV analysis in improving the diagnostic accuracy of PTRPLS. CNVs represent a significant form of genomic variation and should be systematically considered in genetically unresolved Mendelian disorders. Integrating CNV detection algorithms into routine NGS diagnostic workflows has the potential to enhance the identification of pathogenic variants, ultimately facilitating a more comprehensive molecular diagnosis for affected individuals**.**
Keywords: Peters Plus syndrome, Copy number variation, Next-generation sequencing, Mendelian disorders

Enise Avcı Durmuşalioğlu MD, Division of Pediatric Genetics, Department of Pediatrics, School of Medicine, Ege University, Izmir, Turkey
eniseavci.ea@gmail.com, 0000-0002-0582-8881
akcahanbalci@gmail.com, 0000-0001-9770-284X
28.01.2025
27.03.2025
Epub: 10.04.2025

Introduction:
Peters-Plus syndrome (PTRPLS; OMIM #261540) is a rare autosomal recessive congenital disorder of glycosylation caused by mutations in the B3GLCT gene. PTRPLS typically presents with a spectrum of clinical features encompassing ocular defects, disproportionate short stature, clefting and developmental delay (1). Ocular manifestations primarily involve the anterior chamber, with the hallmark being Peters anomaly characterized by corneal clouding and adhesions between the iris, lens, and cornea (2-5). The term 'Peters' Plus syndrome' was introduced in 1984 by Dutch ophthalmologist Mary Van Schooneveld et al., who described 11 patients with anterior eye chamber defects, clefting, short limb dwarfism, and developmental delay (6). Decades later, the molecular etiology was elucidated using genome-wide 1-Mb resolution array-based comparative genomic hybridization and Sanger sequencing, which identified a ∼1.5-Mb interstitial deletion on chromosome 13q12.3q13.1 encompassing the causative gene B3GLCT, along with the common c.660+1G>A variant on the other allele (1). Up to date, splicing, truncating, missense variants, and whole gene deletions have been reported in the B3GLCT (7). B3GLCT plays a crucial role in the modification of proteins, specifically in the process of glycosylation. O-fucose is added to cysteine-rich domains known as thrombospondin type 1 repeats (TSRs) by protein O-fucosyltransferase 2 (POFUT2) and is subsequently elongated with glucose by β3-glucosyltransferase (B3GLCT) (8). Previous studies have indicated that O-linked fucose is crucial for the proper folding and secretion of POFUT2-modified proteins and that the extension of the disaccharide by B3GLCT is vital for only a subset of these targets. Patients with PTRPLS are affected by the reduced function of specific POFUT2/B3GLCT targets, resulting from the loss of B3GLCT activity.
In this study, we aimed to evaluate eleven patients diagnosed with PTRPLS using NGS (Next Generation Sequencing)-based copy number variation (CNV) analysis and to highlight novel molecular approaches that may elucidate the genetic background of rare Mendelian disorders. Traditional techniques, such as microarrays and Multiplex Ligation-dependent Probe Amplification (MLPA), have been commonly

used for CNV detection. However, the introduction of NGS-based CNV analysis has revolutionized the field with its efficiency and cost-effectiveness (9).

Material and Methods:

Patients and samples

The study received approval from the Ethics Committee of Diyarbakir Gazi Yasargil Training and Research Hospital Noninvasive Clinical Research Ethical Committee (approval number: 2024/46). The molecular genetic analysis, including NGS-based CNV analysis, was performed accordingly (10-14). Written informed consent was obtained from their legal parents or guardians, including permission to publish clinical information and photographs of the children. One ophthalmologist and one pediatric genetic specialist evaluated all cases. After a thorough physical examination, dysmorphic features and anthropometric measurements were noted, and Standard Deviations (SD) were accordingly recorded. SD was calculated using a national pediatric calculator following national standards (https://www.ceddcozum.com). Demographic features, family history, clinical and radiographic findings were all obtained from retrospective data. Ophthalmologic examinations were conducted using the following methods: Anterior segment examination was performed with slit-lamp biomicroscopy. Intraocular pressure was measured using an I-care tonometer (I-care Finland Oy, Vantaa, Finland). Pupil dilation was achieved with 1% tropicamide, followed by a detailed fundus examination. For patients whose fundus could not be visualized due to anterior segment pathology, retinal evaluation was performed using B-scan ultrasonography. The clinical diagnosis of PTRPLS was established based on dysmorphic features and molecular genetic results. The demographic and clinical findings of the patients in the present study are summarized in Table 1.

Genetic analysis

Sample Collection: Peripheral blood samples were collected from patients and their family members, and genomic DNA was extracted using the MagNA Pure 96 DNA and Viral NA Small Volume Kit.

Sample Preparation: Clinical exome sequencing (CES) was performed using the Roche HyperCap Designed Share (DS) Inherited Disease Panel kit, covering 4125 genes using the Roche Kapa Hyperexome kit. Samples were prepared following the respective kit protocols, which involved capturing exonic regions of interest using targeted probes.

Sequencing: The prepared CES samples were sequenced on the MGI sequencing platform DNBSEQ-G400. This process generated raw sequencing data as short reads, representing the DNA fragments.

Variant Classification and Analysis: The raw sequencing data (FASTQ files) were uploaded to the SEQ Platform developed by Genomize Inc. The reads were aligned to the human reference genome GRCh37 using the Burrows-Wheeler Aligner (10). Variant calling was performed using FreeBayes (11), followed by additional steps such as PCR deduplication and in-del realignment using Genomize's proprietary algorithms. Identified variants were annotated using VEP v102 (12) to provide functional annotations. American College of Medical Genetics (ACMG) pathogenicity classification was employed using Genomize's proprietary algorithm based on the guideline published by Richards et al. (13).

Copy Number Variation (CNV) Analysis: CNV analysis was conducted using the SEQ Platform from Genomize Inc. Reads aligned to the human reference genome GRCh37 were processed with the GATK gCNV tool v4.1.8.1 (14), using optimized parameters to detect and analyze copy number variations. Additional information from external sources, such as ClinVar entries, bioinformatics-based effect prediction tool scores, and variant frequency values in the SEQ cohort, were considered during the analysis to assess variant significance and frequency further.

Polymerase chain reaction (PCR): Long-range PCR was performed using LongAmp® Taq 2X Master Mix (M0287L, New England Biolabs, NEB) following the manufacturer's protocol. The reaction mixture was prepared in a final volume of 25 µL, containing 13.0 µL LongAmp® Taq 2X Master Mix, 1.0 µL 50 mM $MgCl_2$, 1.0 µL forward primer (B3GLCT-LONG-Y15F: CAACCTCAGCACTTTGGGAG), 1.0 µL reverse primer (B3GLCT-LONG-Y15R: CCCCGGTATCAGTAGAAGGC), 5.0 µL nuclease-free water (ddH_2O), and 80 ng genomic DNA. Thermal cycling conditions included an initial denaturation at 95°C for 5 minutes, followed by 35 cycles of 94°C for 30 seconds (denaturation), 60°C for 1 minute (annealing), and 65°C for 3 minutes (extension), with a final extension at 65°C for 10 minutes and an indefinite hold at 4°C. PCR products were analyzed by agarose gel electrophoresis and visualized under UV light.

Statistical analysis

Data analysis was performed using the Statistical Package for the Social Sciences (SPSS) version 23.0 for Windows (SPSS, Inc., Chicago, IL). Descriptive statistics for quantitative data were presented as arithmetic mean, SD, median, and minimum–maximum values.

Results:

Clinical findings:

Eleven patients (seven male, four female) from six families with a median age at diagnosis of 11.1 ± 12.5 years were included. Five families had first- and/or second-degree consanguineous marriages, and all the families included in the study originated from the same village. Four family pedigrees (F3, F4, F5, F6) were remarkable due to the presence of multiple affected individuals, and five pedigrees (F1, F2, F3, F4, F6) were noteworthy in terms of recurrent abortus and intrauterine termination due to multiple congenital abnormalities, including cleft lip palate and hydrocephaly (Table 1, Supplementary Data 1). All patients were referred to our department due to short stature, facial dysmorphism, and severe brachydactyly. Additionally, except for patients 7, 8, 10, and 11, others exhibited happy facial appearances and muscular body build. At admission, the mean age of the patients was 9.6 ± 13.3 years, ranging from 2 months to 41 years. The mean SD for height and weight at admission were -4.4 ± 0.9 and -3.8 ± 1.8, respectively. The median age at the last evaluation was 11.5 ± 12.3 years. The current mean SD of height, weight, and head circumference were noted -4.1 ± 1.1, -3.1 ± 1.1, -1.9 ± 0.9, respectively. At first examination, all patients displayed similar facial gestalt (Fig. 1 a-k). Three patients (P5, P8 and P9) had cleft lip/palate, which was operated on during infancy (Fig. 1 e, g, j). Interestingly, P9 displayed gingival hypertrophy on the upper incisors (Fig. 1 n). Echocardiography and abdominal ultrasonography were performed in all patients except P11, who had severe joint contractures and intellectual disability, which prevented us from conducting a comprehensive evaluation. Six patients (P3, P5, P6, P7, P9 and P10) exhibited genitourinary abnormalities, including an anteriorly placed anus, deep sacral dimple, and bilateral cryptorchidism. Urinary ultrasonography revealed a duplex collecting system in the left kidney of P10, who subsequently underwent surgery for nephrolithiasis. A skeletal survey was performed in all cases, which revealed no significant findings of skeletal dysplasia apart from severe brachydactyly. P2 was diagnosed with growth hormone deficiency (GHD) based on provocative GH tests (clonidine and L-dopa stimulation) and has been receiving growth hormone treatment for one year, leading to a height increase of 9.5 cm during this period. The Turkish version of the Denver Developmental Screening Test (DDST) was used for patients under five years old, while the Porteus Maze Test (PMT) and Kent EGY test assessed performance and verbal IQ in older patients. Five individuals (P1, P4, P5, P6, P7) exhibited mild developmental delays across fine motor, gross motor, personal-social, and language skills. In contrast, P9 demonstrated a profound global developmental delay in all domains. Additionally, P4 exhibited an attention deficit hyperactivity disorder (ADHD) requiring medical treatment. P2 and P3 exhibited normal intelligence, yet P3 presented with ADHD. P10 showed mild intellectual disability; however, her brother, P11, was compatible with severe mental retardation. Additionally, P7 experienced afebrile seizures from three months of age. Cranial magnetic resonance imaging (MRI) revealed a thin corpus callosum and hydrocephalus in both P7 and P9 (Fig. 2a, b). P9 required a ventriculoperitoneal shunt during the neonatal period. P8, the oldest in the cohort, revealed mild hepatosteatosis and lobulation in the right kidney. Cranial tomography showed enlargement of the third and lateral ventricles, along with atrophy of the hemispheric sulci and fissures. Additionally, a diffuse decrease in the density of the periventricular white matter was noted, which was evaluated as being consistent with chronic ischemic changes (Fig. 2 c, d). He exhibited mild intellectual disability, as he was

unable to learn to read or perform simple mathematical calculations. Moreover, he had been married for six years without having children, suggesting infertility. Elevated follicle-stimulating hormone (FSH) (13.76 mIU/mL) and luteinizing hormone (LH) (10.0 mIU/mL) levels were detected, along with low testosterone (1.59 ng/mL) and antimüllerian hormone (1.60 ng/mL). These findings suggest partial hypergonadotropic hypogonadism. Unfortunately, a spermiogram could not be performed to assess sperm parameters.

Ophtalmologic Findings:

P10 had bilateral central corneal haze with mild to moderate decreased visual acuity and was considered as mild form (Fig. 3 a). P4 had central corneal leucoma covering the pupil and anterior synechiae in the left eye and iris, and retinal coloboma in the right eye (Fig. 3 b). The right eye had cataract surgery and was pseudophakic. P6 displayed right corneal leucoma, prominent iris papillae, and iris and retina coloboma in the same eye (Fig. 3 c). Both P4 and P6 were classified as having a moderate form. P2 and P9 had unilateral corneal leucoma with severe visual loss, corneo-lenticular adhesion, and glaucoma (Fig. 3 d). P9 underwent diode laser treatment twice for glaucoma and is currently on topical latanoprost and dorzolamide-timolol as part of the treatment regimen. P10 and P11, who are siblings, presented with bilateral corneal involvement. However, P11 had more severe involvement in the left eye, leading to vision loss. P1 and P7 exhibited posterior subcapsular opacification, which caused mild visual impairment. P1, P3, and P5 exhibited no corneal opacity but presented with a pale optic disc and chorioretinal atrophy. Additionally, P1 demonstrated crystalline fibrils in the vitreous. P8 had mild corneal haze in one eye, high myopia (-20 diopters), and glaucoma in both eyes. He was using travoprost drops bilaterally. P2, P4, and P5 displayed uni – and/ or bilateral microcornea.

Molecular analysis:

P1 had previously undergone karyotype and chromosomal microarray before presenting to our clinic. We conducted a CES due to the presence of syndromic features and family history suggestive of autosomal recessive inheritance. No pathogenic or likely pathogenic variant related to the phenotype could be detected. However, in all patients, CNV detection algorithms identified a 690 bp homozygous deletion in the 13q12.3 region (hg19: chr13:31903374-31904064), encompassing exon 15 of the B3GLCT (NM_194318.4) gene (Fig. 4 a, c). There were no other morbid OMIM genes except for B3GLCT in the deleted region on chromosome 13q12.3. This alteration found to be Haploinsufficient by Franklin; however, the ClinGen database did not provide reliable data about the haploinsufficiency (HI) score. According to the ACMG criteria, the pathogenicity of this CNV alteration is uncertain and has not been reported in public databases, including DGV and GnomAD. Analysis of BAM files using the Integrative Genomics Viewer (IGV) revealed zero read depth at exon 15 of B3GLCT, despite adequate read depth in control samples sequenced within the same run. Confirmation analysis was planned; however, no specific MLPA probe for B3GLCT was available. Chromosomal microarray analysis had previously failed to identify the deletion. Long-range PCR was considered for confirmation. The nearest exons with sufficient read depth upstream and downstream of exon 15 of B3GLCT were exon 14 of B3GLCT and exon 1 of RXFP2, respectively. Since the exact breakpoints could not be predicted, two long-range PCR reactions using different primer pairs were conducted. NGS-based CNV analysis revealed a decreased read depth in the parents, which indicates a reduced number of sequencing reads aligning with the region of interest. This suggests that the parents are heterozygous carriers of the deletion, as the decreased read depth corresponds to a loss of one copy of the affected genomic region. To demonstrate the carrier status of the patients, primers were designed for the region of interest. We used control, maternal, paternal, and patient samples. The observed PCR amplification in the parents and healthy control indicates the presence of at least one intact allele containing the primer-binding sites, leading to successful amplification. In contrast, no amplification in the patients suggests a homozygous deletion of the target region (Fig. 4 b).

Discussion:

Over the past decade, employing NGS analysis to uncover inherited disorders has significantly expanded our understanding of the genetic basis of Mendelian disorders. NGS enables analysis of multiple regions of the genome in a single reaction and has proven to be a cost-effective and effective tool in the investigation of patients with genetic conditions (15). Unfortunately, it has limitations in its ability to detect CNVs, such as single or multiple exon deletions, which are known to be important contributors to genetic disorders. The application of CNV detection algorithms in NGS diagnostic services can facilitate immediate improvements in the clinical care of individuals with heterogeneous Mendelian disorders (16, 17). P1, the proband of our study, presented with disproportionate short stature and facial dysmorphism and was evaluated for a possible genetic condition; however, despite extensive molecular analyses, including karyotype, microarray, and targeted gene panels, a definitive diagnosis could not be established. Subsequently, ten additional patients, all presenting with nearly identical symptoms, visited our clinic, albeit with varying degrees of clinical severity. NGS-based CNV analysis was subsequently employed to identify significant CNVs that could potentially explain the genetic basis of the condition. All patients were found to harbor a 690 bp homozygous deletion in the 13q12.3 region, covering 15 exons of the B3GLCT gene. The consistent homozygous deletion in exon 15 of the B3GLCT gene across all unrelated patients likely results from a founder effect, as they originate from the same village, indicating a shared common ancestor. This group represents the first report of a homozygous, the smallest exonic deletion in the 13q12.3 region, only encompassing the B3GLCT gene. Other reports have shown that CNV alterations in the same region are causative for PTRPLS, with gene-targeted deletion/duplication analysis identifying four individuals with PTRPLS in the published literature (1, 18, 19). The first deletion was identified by Lesnik-Oberstein using array-based comparative genomic hybridization, revealing a 1.5 Mb interstitial deletion in the 13q12 region of chromosome 13, containing the B3GLCT gene, along with the common c.660+1G>A variant on the other allele in two siblings (1). Similarly, Haldeman-Englert et al. reported a heterozygous 781 kb deletion alongside the common c.660+1G>A variant in a male patient with typical PTRPLS features (19). Comparison of the deletion identified in our study with previous reports reveals a common overlapping region confined to the smallest area of 13q12.3, which includes exon 15th of the B3GLCT gene. Furthermore, while the other two reports documented heterozygous deletions encompassing multiple morbid OMIM genes, this deletion is particularly significant as it is homozygous and represents the smallest deletion reported to date, affecting only the B3GLCT gene. In the literature, documented pathogenic alleles consist of 86% splicing mutations, 6% truncating mutations, 4% missense mutations, and 4% whole gene deletions (7). Therefore, based on our findings and previous studies, we believe that NGS-based CNV analysis plays a crucial role in the diagnosis of genetic variations, including small deletions and duplications associated with inherited Mendelian disorders.

TSRs are present in over 60 human proteins; however, only 49 of these have the required consensus sequence for fucosylation and subsequent modification by B3GLCT, including secreted matrix proteins like thrombospondin-1 (TSP1) and TSP2, as well as all members of the ADAMTS and ADAMTSL families (20). Previous studies have demonstrated that haploinsufficiency of ADAMTS9 and ADAMTS20 is responsible for anterior segment dysgenesis and cardiac anomalies in animal models (21-23). Moreover, both ADAMTS9 and ADAMTS20 play a role in palatal closure, which is the definitive mechanism underlying the observed cleft palate phenotype (21). Furthermore, Adamts20-null mice exhibit a white spotting defect and a high degree of hydrocephalus (24). Mouse B3glct knockout models exhibit craniofacial and skeletal abnormalities similar to those observed in PTRPLS patients (24). These independent observations collectively suggest that PTRPLS specifically results from secretion defects in certain target proteins of B3GLCT (25). In addition, loss of B3GLCT significantly reduces the secretion of ADAMTSL2 (25). Geleophysic dysplasia (GD), caused by mutations in ADAMTSL2 leading to reduced secretion of the mutant protein compared to the wild-type protein, shares several common symptoms with PTRPLS (25, 26). In our cohort, P1, P2, P3, and P5 were initially diagnosed with GD based on severe brachydactyly, muscular body build, and a characteristic happy facial appearance. However, severe cardiac involvement in GD and distinct ocular findings in PTRPLS may provide valuable clinical clues for distinguishing between the two phenotypes. Consequently, comprehensive evaluation of both systems is essential, and we recommend considering PTRPLS in individuals who test negative for GD mutations.

Affected individuals present with similar phenotypes and complaints, yet there is significant intra-and interfamilial variability (1, 19). In our study, we noted phenotypic variability consistent with previous reports on PTRPLS. The study by Oberstein et al. highlighted that even within a genetically homogeneous group (homozygous for c.1020-1G>A), cognitive outcomes ranged from normal secondary education to severe cognitive impairment, suggesting the influence of additional genetic or environmental modifiers (1). Similarly, Haldeman-Englert et al. proposed that the variable phenotypes in patients with deletions involving B3GLCT may result from the multisystemic effects of glycosylation defects or the involvement of other genes within the deleted region (19). Furthermore, no clear genotype-phenotype correlation has been established to date, and the cause of intra- and interfamilial variability remains unknown. It is likely that factors beyond the primary genetic variant, such as modifier genes, epigenetic influences, or environmental factors, contribute to the phenotypic heterogeneity observed in PTRPLS. Ophthalmologic anomalies, which can provide clues for an accurate diagnosis, have emerged as another feature that demonstrates this variability in this study. Four patients (P1, P3, P5, and P7) did not exhibit anterior segment dysgenesis or Peters anomaly. However, they all presented with retinal atrophy, except for P7. Ocular involvement is generally bilateral; however, unilateral cases have also been reported (27). Consistent with the literature, Peters anomaly was observed bilaterally in 5 of our patients and unilaterally in 2. Cataract and glaucoma, common features that can also occur later in life, were observed in 6 out of 11 patients in our cohort. Interestingly, unusual eye symptoms, including severe myopia, iris coloboma, retinal coloboma, optic atrophy, and microcornea, were noted in 9 patients. Cardiac involvement is another systemic feature that varies among affected individuals. Congenital heart defects occur in approximately 30% of cases (1). Consistent with the literature, we observed bicuspid aorta, ASD, VSD, patent foramen ovale (PFO), and pulmonary stenosis in 4 out of 11 patients (36%).

Despite severe short stature, the skeletal survey showed no definitive evidence of skeletal dysplasia, apart from brachydactyly. Our observations suggest that brachydactyly was more pronounced in patients under five years of age than in older individuals. In the context PTPRLS, GH therapy has been shown to yield positive results in a limited number of cases. Three reports in the literature have described patients with PTRPLS who demonstrated a good response to GH therapy. In these cases, GH deficiency was identified, which may have contributed to the patients' short stature. However, in all three studies, the molecular diagnoses of the patients were not established; instead, the diagnosis of PTRPLS was based on clinical findings. One of these reports also highlighted that pituitary dysfunction is well known to be associated with midline defects, encompassing a broad spectrum of congenital midline anomalies. These range from severe, nonviable conditions to milder presentations, such as isolated cleft lip or palate, as observed in PTRPLS. Notably, the prevalence of GH deficiency is reported to be 40 times higher in children with cleft lip and palate or isolated cleft palate compared to those without such anomalies. This strong correlation between pituitary dysfunction and congenital craniofacial malformations suggests that every child with midline facial defects should undergo a pituitary evaluation (28-30). Another study reported two siblings diagnosed with PTRPLS who also had GH deficiency and a small pituitary gland, yet no variants were detected in the B3GLCT gene (30). This highlights the importance of performing cranial MRI in patients with GH deficiency and underscores the need to investigate CNVs in cases negative for B3GLCT variants. In our cohort, only P2 exhibited GH deficiency. Treatment with recombinant GH resulted in an increased growth velocity (9.5 cm/year), improving height from -4.0 to -3.3 SDS over one year of therapy, indicating a promising outcome. However, as demonstrated by previous reports of GH deficiency in children with PTRPLS, a pituitary evaluation should be considered, particularly in the presence of midline facial defects, and the growth hormone/insulin-like growth factor axis should be assessed. Further studies with larger cohorts are needed to better understand the prevalence of GH deficiency in PTRPLS, the long-term benefits of GH therapy, and its potential role in managing growth impairments in this population.

In our cohort, four patients were over the age of 10, and only one of them, P8 (40 years old), was diagnosed with partial hypergonadotropic hypogonadism. This diagnosis was based on elevated gonadotropin levels (FSH and LH) alongside low testosterone and antimüllerian hormone levels. To our knowledge, hypergonadotropic hypogonadism has not been previously reported in patients with PTRPLS. This raises the question of whether it represents an unrecognized feature of the syndrome or an unrelated coexisting condition. Further studies involving additional patients are needed to clarify this association. However, we recommend monitoring patients for hypogonadism as they age.

Limitations

A limitation of the study is the inability to determine the exact breakpoints of the suspected deletion using an alternative method. However, the amplification failure of LR-PCR indirectly indicated the deletion. Furthermore, the suspected deletion was identified in all patients and their parents through NGS-based CNV analysis.

In conclusion, previous studies have demonstrated that CNVs can contribute to the pathogenesis of PTRPLS. Deletions involving the B3GLCT gene can result in a clinical phenotype similar to that caused by point mutations within the gene. These findings highlight the importance of CNVs, especially in cases where standard genetic testing fails to detect small deletions/duplications. The accurate detection of CNVs using this method highlights its value as a powerful tool in genetic diagnostics. Consequently, our study emphasizes the importance of incorporating NGS-based CNV analysis into routine genetic testing, which may lead to better clinical outcomes and personalized management for individuals with Mendelian disorders.

Acknowledgments

We thank our patients and their families for their collaboration and participation, and we are thankful to Aşkın Özel for his technical support.

Authors' contributions

AA, EA, TA, and EI were responsible for the acquisition, analysis, and interpretation of data and drafting of the manuscript. AA, EÜ, TA, and EI were responsible for project conceptualization, analysis, and interpretation of data and critical review of the manuscript. AA, EÜ, TA, TTT and YCD were responsible for the analysis and interpretation of data and critical review of the manuscript. ŞÖ, RK, LH, VÖ, and EI were responsible for the critical review of the manuscript. TA, ÖÇ, and EI were the chief investigators, responsible for the conception and design of the work, acquisition, analysis, and interpretation of data; and writing of the manuscript. All authors gave final approval of the version to be published and agreement to be accountable for all aspects of the work.

Funding

The authors declare that no funds, grants, or other support were received during the preparation of this manuscript.

Data availability

The data supporting this study's findings are available upon request from the corresponding author. The data are not publicly available due to privacy or ethical restrictions. Artificial intelligence (AI) and AI-assisted technologies were not employed in the preparation of this manuscript.

Declarations

Ethical approval This study was performed in line with the principles of the Declaration of Helsinki. Approval was granted by Health Sciences, Diyarbakir Gazi Yasargil Training and Research Hospital Noninvasive Clinical Research Ethical Committee (approval number: 2024/46).

Consent to participate Written informed consent was obtained from the parents.

Conflict of Interest The authors declare no conflict of interests.

Acknowledgments

This study was performed in line with the principles of the Declaration of Helsinki. The study received approval from the Ethics Committee of Diyarbakir Gazi Yasargil Training and Research Hospital Noninvasive Clinical Research Ethical Committee (approval number: 2024/46). We thank our patients and their families for their collaboration and participation, and we are thankful to Aşkın Özel for his technical support.

References

1. Oberstein SAL, Kriek M, White SJ, Kalf ME, Szuhai K, den Dunnen JT, et al. Peters Plus syndrome is caused by mutations in B3GALTL, a putative glycosyltransferase. The American Journal of Human Genetics. 2006;79(3):562-6.
2. Hennekam R, editor The Peters' plus syndrome: a review. Annales de genetique; 2002.
3. Shah PR, Chauhan B, Chu CT, Kofler J, Nischal KK. Ocular phenotype of peters-plus syndrome. Cornea. 2022;41(2):219-23.
4. Zaidman GW, Flanagan JK, Furey CC. Long-term visual prognosis in children after corneal transplant surgery for Peters anomaly type I. American journal of ophthalmology. 2007;144(1):104-8. e1.
5. Bhandari R, Ferri S, Whittaker B, Liu M, Lazzaro DR. Peters anomaly: review of the literature. Cornea. 2011;30(8):939-44.
6. Van Schooneveld M, Delleman J, Beemer F, Bleeker-Wagemakerp E. Peters'-plus: a new syndrome. Ophthalmic paediatrics and genetics. 1984;4(3):141-5.
7. Weh E, Reis LM, Tyler RC, Bick D, Rhead WJ, Wallace S, et al. Novel B3GALTL mutations in classic Peters plus syndrome and lack of mutations in a large cohort of patients with similar phenotypes. Clinical genetics. 2014;86(2):142-8.
8. Heinonen TY, Mäki M. Peters'-plus syndrome is a congenital disorder of glycosylation caused by a defect in the β1, 3-glucosyltransferase that modifies thrombospondin type 1 repeats. Annals of medicine. 2009;41(1):2-10.
9. Royer-Bertrand B, Cisarova K, Niel-Butschi F, Mittaz-Crettol L, Fodstad H, Superti-Furga A. CNV detection from exome sequencing data in routine diagnostics of rare genetic disorders: opportunities and limitations. Genes. 2021;12(9):1427.
10. Li H, Durbin R. Fast and accurate short read alignment with Burrows–Wheeler transform. bioinformatics. 2009;25(14):1754-60.
11. Garrison E, Marth G. Haplotype-based variant detection from short-read sequencing. arXiv preprint arXiv:12073907. 2012.
12. McLaren W, Gil L, Hunt SE, Riat HS, Ritchie GR, Thormann A, et al. The ensembl variant effect predictor. Genome biology. 2016;17:1-14.
13. Richards S, Aziz N, Bale S, Bick D, Das S, Gastier-Foster J, et al. Standards and guidelines for the interpretation of sequence variants: a joint consensus recommendation of the American College of Medical Genetics and Genomics and the Association for Molecular Pathology. Genetics in medicine. 2015;17(5):405-23.
14. Babadi M, Fu JM, Lee SK, Smirnov AN, Gauthier LD, Walker M, et al. GATK-gCNV enables the discovery of rare copy number variants from exome sequencing data. Nature genetics. 2023;55(9):1589-97.
15. Jamuar SS, Tan E-C. Clinical application of next-generation sequencing for Mendelian diseases. Human genomics. 2015;9:1-6.
16. Ellingford JM, Campbell C, Barton S, Bhaskar S, Gupta S, Taylor RL, et al. Validation of copy number variation analysis for next-generation sequencing diagnostics. European Journal of Human Genetics. 2017;25(6):719-24.
17. Atik T, Avci Durmusalioglu E, Isik E, Kose M, Kanmaz S, Aykut A, et al. Diagnostic yield of exome sequencing-based copy number variation analysis in Mendelian disorders: a clinical application. BMC Medical Genomics. 2024;17(1):239.
18. Kapoor S, Mukherjee SB, Arora R, Shroff D. Peters plus syndrome. The Indian Journal of Pediatrics. 2008;75:635-7.
19. Haldeman-Englert CR, Naeem T, Geiger EA, Warnock A, Feret H, Ciano M, et al. A 781-kb deletion of 13q12. 3 in a patient with Peters plus syndrome. American journal of medical genetics Part A. 2009;149(8):1842.
20. Du J, Takeuchi H, Leonhard-Melief C, Shroyer KR, Dlugosz M, Haltiwanger RS, et al. O-fucosylation of thrombospondin type 1 repeats restricts epithelial to mesenchymal transition (EMT) and maintains epiblast pluripotency during mouse gastrulation. Developmental biology. 2010;346(1):25-38.
21. Enomoto H, Nelson CM, Somerville RP, Mielke K, Dixon LJ, Powell K, et al. Cooperation of two ADAMTS metalloproteases in closure of the mouse palate identifies a requirement for versican proteolysis in regulating palatal mesenchyme proliferation. Development. 2010;137(23):4029-38.
22. Dubail J, Vasudevan D, Wang LW, Earp SE, Jenkins MW, Haltiwanger RS, et al. Impaired ADAMTS9 secretion: A potential mechanism for eye defects in Peters Plus Syndrome. Scientific reports. 2016;6(1):33974.
23. Kern CB, Wessels A, McGarity J, Dixon LJ, Alston E, Argraves WS, et al. Reduced versican cleavage due to Adamts9 haploinsufficiency is associated with cardiac and aortic anomalies. Matrix biology. 2010;29(4):304-16.
24. Holdener BC, Percival CJ, Grady RC, Cameron DC, Berardinelli SJ, Zhang A, et al. ADAMTS9 and ADAMTS20 are differentially affected by loss of B3GLCT in mouse model of Peters plus syndrome. Human molecular genetics. 2019;28(24):4053-66.
25. Vasudevan D, Takeuchi H, Johar SS, Majerus E, Haltiwanger RS. Peters plus syndrome mutations disrupt a noncanonical ER quality-control mechanism. Current biology. 2015;25(3):286-95.
26. Le Goff C, Morice-Picard F, Dagoneau N, Wang LW, Perrot C, Crow YJ, et al. ADAMTSL2 mutations in geleophysic dysplasia demonstrate a role for ADAMTS-like proteins in TGF-β bioavailability regulation. Nature genetics. 2008;40(9):1119-23.
27. Oberstein SAL, Ruivenkamp CA, Hennekam RC. Peters Plus Syndrome. GeneReviews®[Internet]. 2017.
28. Lee KW, Lee PD. Growth hormone deficiency (GHD): a new association in Peters' Plus syndrome (PPS). American Journal of Medical Genetics Part A. 2004;124(4):388-91.
29. de Buy Wenniger LJM, Hennekam RC, editors. The Peters' plus syndrome: a review. Annales de genetique; 2002: Elsevier.
30. Al-Gazali L, Shather B, Kaplan W, Algawi K, Ali BR. Anterior segment anomalies of the eye, growth retardation associated with hypoplastic pituitary gland and endocrine abnormalities: Jung syndrome or a new syndrome? American Journal of Medical Genetics Part A. 2009;149(2):251-6.

Fig 1. Photographs of older patients in the study. a) P2 (11 years and 8 months), b) P3 (10 years), c) P10 (15 years and 9 months), d) P11 (26 years), and e) P8 (41 years). Common dysmorphic features include hypertelorism, a high anterior hairline, a thin vermillion border with a Cupid's bow-shaped upper lip, and a long philtrum. Additionally, P2, P10 and P11 displayed low-set ears (a, c d), while P3 exhibited up-slanting palpebral fissures (b).
Second row: Photographs of patients under six years old. f) P1 (3 years and 8 months), g) P5 (3 years and 2 months), h) P4 (5 years and 5 months), i) P6 (3 years and 7 months), j) P9 (4 years and 9 months), and P7 (2 months). All patients exhibit nearly identical facial features, including hypertelorism, a long philtrum, low-set ears, and a thin vermillion border. Note the short neck and muscular body build, which overlap with features of geleophysic dysplasia. Hands are notably short with brachydactyly. P5 and P9 had cleft lip/palate repair surgery (g, j).
Third row: Characteristic findings of PTRPLS in the present study. P4 had corneal clouding in the left eye (l). P9 exhibited severe glaucoma in the left eye, resulting in vision loss, and underwent surgeries for both glaucoma and cleft lip/palate (m). Additionally, P9 displayed remarkable gingival hypertrophy, an uncommon feature of PTRPLS (n). P6 had an ear pit and low-set, posteriorly rotated ears (o).

Fig 2. MRI findings of Patient 7. Widened lateral ventricles (indicated by red arrows) and a cavum septum pellucidum vergae variant (highlighted by a yellow arrow) were observed (a). Corpus callosum hypoplasia (red arrow) was seen in the sagittal section (b). CT imaging of Patient 8. The ventricular system and sulci appeared widened (red arrows), indicating cerebral atrophy (c,d). Additionally, a diffuse decrease in periventricular white matter density was observed, consistent with chronic ischemic changes (d).

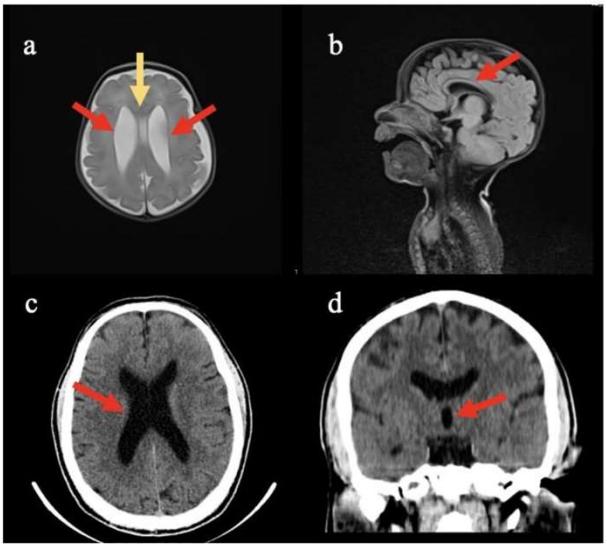

Fig. 3. Ophthalmologic abnormalities detected in the study a) Patient 10; corneal haze, b) Patient 4; central corneal leucoma covering the pupil and anterior synechiae (left photo) and iris coloboma and pseudophakic (right photo). c) Patient 6; central corneal leucoma and iris coloboma. d) Patient 2; central and nasal paracentral corneal leucoma with corneo-lenticular adhesion

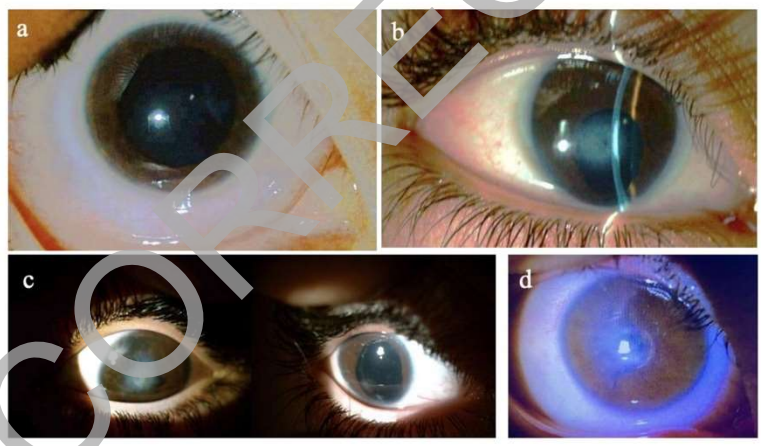

Fig 4. NGS-based CNV analysis. a) CNV alteration of the two probands on the IGV vizulation. While controls demonstrated no alteration of CNV, the first and second rows show the O copy number of the 15th exons of the B3GLCT gene. b) Given that the parents are known to be first cousins and predicted to be obligatory heterozygous carriers of the deletion, the detected amplicons in their PCR reactions are likely derived from their non-deleted, healthy alleles. This assumption is supported by the fact that the healthy control, possessing two non-deleted alleles, also showed similar amplification. c) NGS-based CNV analysis through CES revealed a decreased read depth in the parental samples, indicative of a potential heterozygous deletion.
C: control, F: father, M: mother, P6: patient 6, P8: Patient8